JOURNAL OF GUIDANCE, CONTROL, AND DYNAMICS
Vol. 28, No. 1, January–February 2005

Model Updating Using the Closed-Loop Natural Frequency

Hunsang Jung* and Youngjin Park†
Korea Advanced Institute of Science and Technology, Daejon 305-701, Republic of Korea

Parameter modification of a linear finite element model (FEM) based on a modal sensitivity matrix is usually performed through an effort to match FEM modal data to experimental ones. However, there are cases where this method cannot be applied successfully; lack of reliable modal data and ill-conditioning of the modal sensitivity matrix constitute such cases. In this research, a novel concept of introducing feedback loops to the conventional modal test setup is proposed. This method uses closed-loop natural frequency data for parameter modification to overcome the problems associated with the conventional method based on modal sensitivity matrix. The feedback loop changes the modal characteristics of the system, and the closed-loop natural frequencies can be used as additional information to solve the problem caused by lack of reliable modal data. Through proper selection of exciter and sensor locations and associated feedback gains, the condition number of the modal sensitivity matrix can be reduced, and a more reliable estimation result can be expected. A parameter modification scheme based on the closed-loop natural frequency data along with the modal sensitivity modification and controller design method is explained. Proposed controller design method is efficient in changing modes. Numerical simulation of parameter estimation based on time-domain input/output data is provided to demonstrate the estimation performance of proposed method.

I. Introduction

THE well-known problem of making a reliable model of a flexible structure can be categorized into direct and indirect methods. The system matrix updated using the direct method can contain off-diagonal terms indicating a physically impossible structure and sometimes loses the positive definiteness as a result of incompleteness of the measured mode shapes. To overcome such drawbacks of the direct approach, an indirect method based on the modal or frequency-response-function (FRF) sensitivity to parameter perturbation has been developed by many researchers.[1,2] The difference in modal information between model and system are used to estimate suspicious parameters such as joint stiffness of the initial finite element model (FEM). This way, positive definiteness of mass and stiffness matrices developed through the use of FEM is guaranteed while keeping the original structure of FEM intact. This method encounters two well-known problems[1,2]: the lack of reliable modal data and ill conditioning of the modal sensitivity matrix.

The problem of lacking reliable modal data should be considered first. It is known that natural frequency estimation from measurement data carries less errors because a natural frequency is estimated using all measured FRFs, whereas an element of mode-shape vector is calculated from single FRF. Actually, it is reported that errors in natural frequency estimation from measured data can be reduced to less than 1% without much difficulty, whereas those in mode-shape measurement can be in the range of 10%, according to some experimental results.[3] The measured modal data are of complex values because structural system carries damping, which usually induces complex modal data. To correlate the modal data of system and model, measured complex modal data should be transformed to normal modal data because we can obtain only normal modal data from FEM where damping information is not included. Excluding the case of proportional damping, normal mode shape from measurement data always includes errors. The bias error contained in normal mode-shape measurement induces relatively large bias errors in estimated parameters and consequently degrades the confidence of the updated model. If all of the unreliable mode-shape measurement data are discarded, remaining modal data are insufficient to estimate all of the necessary parameter updates. In this case, the number of the updating parameters should be reduced in the conventional method. Attempts to increase the natural frequency measurements in the absence of error-contaminated mode-shape measurements have been carried out by many researchers. W. D'ambrogio et al.[4] suggested a method that includes antiresonance points in model updating, and S. Li et al.[5] increased the natural frequency measurements by changing the boundary conditions of a system. Similarly, N. Nalitolela et al.[6] suggested a method to add a point mass or point stiffness to measure additional natural frequencies of a perturbed system, and recently P. D. Cha et al.[7] implemented this idea to obtain the unique solution of updating parameters. J. H. Gordis et al.[8] and N. Nalitolela et al.[9] suggested a methodology based on imaginary boundary conditions. Recently J. S. Lew and Juang[10] adopted an externally imposed feedback loop using collocated sensor and actuator to increase the modal information. Collocated sensor and actuator can increase the modal information without destabilizing the system. However, all of these approaches have the following drawbacks: The antiresonance points are linearly dependent to the natural frequencies, and the number of measurable antiresonance points is limited. The addition of a point mass or point stiffness is useful in increasing the modal data, but difficulties can arise in actual implementation as a result of limits on system modification. The additional natural frequency data produced by the use of imaginary boundary conditions are not obtained through additional experiments but constructed using measured FRFs. Small bias errors in measured FRFs can cause large bias errors in modified FRFs around the new natural frequencies. The feedback method using collocated sensor and exciter set can bring no more than the same effect of point mass and point stiffness method to system. They did not consider the case of noncollocated sensor and exciter set in which the system can be changed in more diverse ways but guaranteeing of system stability becomes an issue. In this research, we basically deal with the controller design of noncollocated sensor and exciter set and propose a method to maintain the stability of closed-loop system through the weighting matrix adjustment of controller design performance index.

Ill conditioning of the modal sensitivity matrix can also contribute to inaccurate model updating. Ill conditioning of the sensitivity matrix comes from the fact that the eigendata or FRF sensitivities of some updating parameters are similar to one another and the difference of those parameters cannot be distinctly determined

Received 28 July 2003; revision received 5 February 2004; accepted for publication 9 February 2004.

*Graduate Student, Department of Mechanical Engineering, Science Town; elrond@kaist.ac.kr.

†Professor, Department of Mechanical Engineering, Science Town; yjpark@mail.kaist.ac.kr.

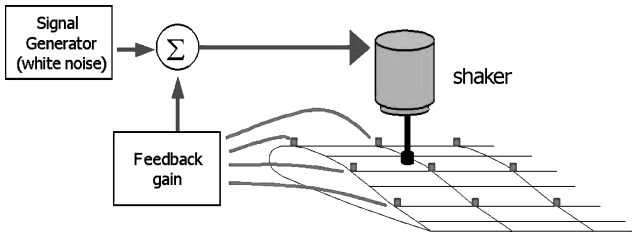

Fig. 1 Concept of feedback loop.

by the use of conventional sensitivity-based methods. This problem cannot be solved easily without changing the modal characteristics of the original system. The previous research[1,2,11] on this subject mainly focused on preventing the updating parameters from diverging during iteration.

To overcome such drawbacks of the indirect approach, we propose a new method that introduces feedback loops from the sensors to the exciter of the conventional modal test setup as shown in Fig. 1. The modal data of the closed-loop system change from the original data as a result of feedback loops. This modal change can serve as additional information for system identification. Measurements of the closed-loop mode shapes are excluded because they carry relatively larger errors than closed-loop natural frequencies do. Changing sensor and exciter locations and corresponding feedback gains can generate various closed-loop natural frequencies. By using all of these natural frequency changes, the shortage of reliable modal measurements can be overcome. Ill conditioning of the modal sensitivity matrix can also be resolved as modal sensitivity of the parameters to update are changed by feedback. In this paper, the process of parameter estimation using the closed-loop natural frequency measurements is explained. Modification of the modal sensitivity matrix and the design criterion of the control loop are discussed. Simulation examples are provided to explain the modified parameter estimation process and the proposed control method. And parameter estimation errors according to data number are provided to demonstrate the performance of the proposed method compared to the conventional method based on open-loop modal data.

II. System Description and Basic Updating Procedure

The linear-time-invariant model of a vibrating structure is described as follows:

$$\boldsymbol{M}\ddot{\boldsymbol{x}} + \boldsymbol{C}\dot{\boldsymbol{x}} + \boldsymbol{K}\boldsymbol{x} = \boldsymbol{f} = \boldsymbol{b}f \tag{1}$$

$$\boldsymbol{b}(i) = \begin{cases} 1 & \text{if} \quad i = a \\ 0 & \text{if} \quad i \neq a \end{cases} \tag{2}$$

where a indicates the exciter position. The modal data of this system satisfy the following properties:

$$\boldsymbol{K}W = \boldsymbol{M}W\Lambda \tag{3}$$

$$W^T\boldsymbol{M}W = I, \qquad W^T\boldsymbol{K}W = \Lambda \tag{4}$$

$$W = [W_1 \quad W_2 \quad \cdots \quad W_n], \qquad \Lambda = \text{diag}[\lambda_i], \qquad \lambda_i = \omega_i^2 \tag{5}$$

where Λ and W are $n \times n$ matrices of eigenvalues and eigenvectors, respectively. Each eigenvalue is the square of a natural frequency as shown in Eq. (5). W is orthonormal to the mass and stiffness matrices as shown in Eq. (4).

$\boldsymbol{M}$ and $\boldsymbol{K}$, which we want to update, can be described as the summation of initial values from FEM, $\boldsymbol{M}_0$ and $\boldsymbol{K}_0$, and their first perturbations with respect to updating parameters.

$$\boldsymbol{M} = \boldsymbol{M}_0 + \sum_{j=1}^{l} \delta\theta_j \frac{\partial \boldsymbol{M}}{\partial \theta_j} \tag{6}$$

$$\boldsymbol{K} = \boldsymbol{K}_0 + \sum_{j=1}^{l} \delta\theta_j \frac{\partial \boldsymbol{K}}{\partial \theta_j} \tag{7}$$

where θ_j and l are the updating parameters and their total number, respectively. $\partial\boldsymbol{M}/\partial\theta_j$ and $\partial\boldsymbol{K}/\partial\theta_j$ can be viewed as sensitivity of mass and stiffness to updating parameters, respectively. These matrices can be computed from some initial model such as FEM. The eigenvalue sensitivity of given updating parameter for the linear system model with distinct eigenvalues is given as follows[1]:

$$\frac{\partial \lambda_t}{\partial \theta_j} = W_t^T \left[\frac{\partial \boldsymbol{K}}{\partial \theta_j} - \lambda_t \frac{\partial \boldsymbol{M}}{\partial \theta_j} \right] W_t \tag{8}$$

$$\boldsymbol{S} = \left[\frac{\partial \lambda_t}{\partial \theta_j} \right] \tag{9}$$

where $\boldsymbol{S}$ is eigenvalue sensitivity matrix and subscript t is used to represent target mode. If the difference between system and its initial model can be expressed as a first-order perturbation with respect to updating parameters, the modal data discrepancy between system and model is linearly related to the parameter perturbation.

$$\delta z = \boldsymbol{S}\delta\boldsymbol{p} \tag{10}$$

where $\delta\boldsymbol{p} = \boldsymbol{p}_r - \boldsymbol{p}$, $\delta z = z_r - z$, $\boldsymbol{p}$ is the updating parameter vector, and z is the eigenvalue vector of model, respectively. Symbols with the subscript $\boldsymbol{r}$ represent the actual system properties. Modal data of system are complex-valued data because the damping of system induces the phase variation in modal data. We have to use normalized modal data to correlate with normal modal data of FEM, and z_r is a normalized modal data from complex modal data. Using the following performance index, parameters are estimated to minimize the difference between z and z_r.

$$J(\delta\boldsymbol{p}) = (\delta z - \boldsymbol{S}\delta\boldsymbol{p})^T(\delta z - \boldsymbol{S}\delta\boldsymbol{p}) \tag{11}$$

Least-square solution of this problem is obtained using the generalized inverse as follows:

$$\delta\boldsymbol{p} = \boldsymbol{S}^{+}\delta z \tag{12}$$

In general, iterative parameter estimation is used to compensate for the nonlinearity of the relation between the updated parameters and the modal data. If the variance information of the measurement noise is available, statistical solvers such as minimum variance estimation can be used in parameter estimation, and the noise effect on estimated parameters can be minimized.

III. Parameter Estimation Procedure Using Closed-Loop Modal Data

A parameter estimation procedure using closed-loop modal data is proposed. To use the closed-loop modal data, the governing equation for the linear-time-invariant system and its modal sensitivity matrix are modified considering exciter dynamics and feedback loop.

A. Formulation of the Closed-Loop System

Figure 2 shows the conceptual diagram of the proposed feedback method. Adding sensor signals to the exciter reference signal generates the feedback loop. In a conventional modal test, the output and input signals are measured using accelerometers and a force transducer located at the stinger tip of an exciter. Such an input-output configuration corresponds to positions (b) and (c) in Fig. 2. In the closed-loop system, the input–output configuration is changed to positions (a) and (c) in Fig. 2. In this case, the exciter is included in

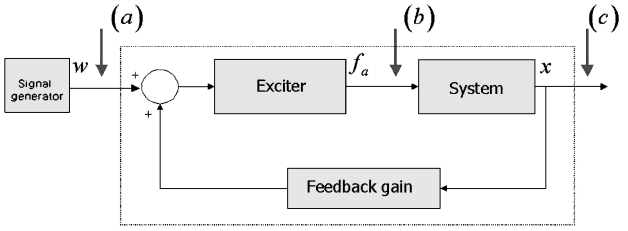

Fig. 2 Concept of feedback loop.

closed-loop system, and its dynamics should be modeled. The mechanical part of the electromagnetic exciter comprises the armature mass and the spring.

$$m_a\ddot{x}_a + c_a\dot{x}_a + k_a x_a + f_a = f_e \tag{13}$$

where m_a, k_a, c_a, and x_a are armature mass, spring stiffness, damping, and armature displacement, respectively. The electromagnetic force f_e vibrates the armature mass and transmits the excitation force f_a to the target structure through a stinger connection. Equation (13) can be denoted using the displacement vector of the system as follows:

$$\boldsymbol{m}_a\ddot{\boldsymbol{x}} + \boldsymbol{c}_a\dot{\boldsymbol{x}} + \boldsymbol{k}_a\boldsymbol{x} + f_a = f_e \tag{14}$$

where $\boldsymbol{m}_a$ is a row vector whose elements are zero except the ath element, which is m_a. Structures of $\boldsymbol{c}_a$ and $\boldsymbol{k}_a$ follow the same pattern. The input to this exciter is the summation of the exciter reference signal and the output signals multiplied with proper gains. We confine the type of the controller to static output feedback control for design simplicity.

$$f_e = \mu_F(\boldsymbol{r} - \boldsymbol{k}_f\boldsymbol{x} - \boldsymbol{c}_f\dot{\boldsymbol{x}} - \boldsymbol{m}_f\ddot{\boldsymbol{x}}) \tag{15}$$

where r is the exciter reference signal and $\boldsymbol{k}_f$, $\boldsymbol{c}_f$, and $\boldsymbol{m}_f$ are the feedback gains for displacement, velocity, and acceleration measurements, respectively; μ_F is used to express the dynamics of the exciter amp. As the dynamics of the electric circuit become faster than that of the mechanical part, μ_F can be assumed as a constant value over the operating frequency range. By adding Eqs. (14) and (15) to Eq. (1), the following linear model for closed-loop system can be obtained:

$$(\boldsymbol{M} + \boldsymbol{b}\boldsymbol{m}_a + \mu_F\boldsymbol{b}\boldsymbol{m}_f)\ddot{\boldsymbol{x}} + (\boldsymbol{C} + \boldsymbol{b}\boldsymbol{c}_a + \mu_F\boldsymbol{b}\boldsymbol{c}_f)\dot{\boldsymbol{x}}$$
$$+ (\boldsymbol{K} + \boldsymbol{b}\boldsymbol{k}_a + \mu_F\boldsymbol{b}\boldsymbol{k}_f)\boldsymbol{x} = \mu_F\boldsymbol{b}r \tag{16}$$

Original mass, damping, and stiffness matrices are added with the exciter dynamics and feedback gain matrices. Armature mass and spring stiffness of the exciter can be easily measured. Then we can change the system by adjusting the feedback gains. Note that the symmetry in each of the mass, damping, and stiffness matrices is lost by the use of the feedback loop. This asymmetry in the system matrices requires some modification in the updating procedure as the conventional computation of the modal sensitivity matrix relies on symmetry of the mass and stiffness matrices.

B. Modified Updating Procedure

The mass and stiffness matrices after the feedback loop are as follows:

$$\boldsymbol{M}_f = \boldsymbol{M}_0 + \boldsymbol{b}\boldsymbol{m}_a + \mu_F\boldsymbol{b}\boldsymbol{m}_f \tag{17}$$

$$\boldsymbol{K}_f = \boldsymbol{K}_0 + \boldsymbol{b}\boldsymbol{k}_a + \mu_F\boldsymbol{b}\boldsymbol{k}_f \tag{18}$$

For asymmetric system matrices, the left and right eigenvectors corresponding to the same eigenvalue are not identical, and the following biorthogonality holds:

$$\boldsymbol{K}_f W^R = \boldsymbol{M}_f W^R \Lambda \tag{19}$$

$$\boldsymbol{K}_f^T W^L = \boldsymbol{M}_f^T W^L \Lambda \tag{20}$$

$$(W^L)^T\boldsymbol{K}_f W^R = \Lambda, \qquad (W^L)^T\boldsymbol{M}_f W^R = I \tag{21}$$

where W^L and W^R are the left and right eigenvectors, respectively. Equation (21) is the description of the biorthogonality. The modified eigenvalue sensitivity with respect to updating parameters based on the biorthogonality is as follows:

$$\frac{\partial_c\lambda_t}{\partial\theta_j} = \left(W_t^L\right)^T\left[\frac{\partial\boldsymbol{K}_f}{\partial\theta_j} - {}_c\lambda_t\frac{\partial\boldsymbol{M}_f}{\partial\theta_j}\right]W_t^R \tag{22}$$

Though system matrix symmetry does not hold, the sensitivity matrix can be obtained by computing the left and right eigenvectors of the closed-loop model. Refer to the Appendix for a detailed derivation. Based on this modified sensitivity matrix, the linear relationship between updating parameter and modal data can be represented as follows:

$$\boldsymbol{z}_r^i - \boldsymbol{z}^i = \boldsymbol{S}^i\delta\boldsymbol{p} \tag{23}$$

where superscript i is used to represent the closed-loop eigenvalue and its sensitivity matrix using ith feedback loop setup. The closed-loop eigenvalues for many feedback control settings are added to the performance index.

$$J(\delta\boldsymbol{p}) = (\delta\boldsymbol{z}^0 - \boldsymbol{S}^0\delta\boldsymbol{p})^T(\delta\boldsymbol{z}^0 - \boldsymbol{S}^0\delta\boldsymbol{p}) + (\delta\boldsymbol{z}^1 - \boldsymbol{S}^1\delta\boldsymbol{p})^T(\delta\boldsymbol{z}^1 - \boldsymbol{S}^1\delta\boldsymbol{p})$$
$$+ \cdots + (\delta\boldsymbol{z}^k - \boldsymbol{S}^k\delta\boldsymbol{p})^T(\delta\boldsymbol{z}^k - \boldsymbol{S}^k\delta\boldsymbol{p}) = (\delta\boldsymbol{z} - \boldsymbol{T}\delta\boldsymbol{p})^T(\delta\boldsymbol{z} - \boldsymbol{T}\delta\boldsymbol{p}) \tag{24}$$

where $\boldsymbol{T}$ and $\delta\boldsymbol{z}$ are defined as

$$\boldsymbol{T}^T = [(\boldsymbol{S}^0)^T(\boldsymbol{S}^1)^T \quad \cdots \quad (\boldsymbol{S}^k)^T]$$
$$\delta\boldsymbol{z}^T = \left[\left(\boldsymbol{z}_r^0 - \boldsymbol{z}^0\right)^T\left(\boldsymbol{z}_r^1 - \boldsymbol{z}^1\right)^T \quad \cdots \quad \left(\boldsymbol{z}_r^k - \boldsymbol{z}^k\right)^T\right] \tag{25}$$

The minimization of the performance index in Eq. (24) requires the following matrix inverse problem solved:

$$\boldsymbol{T}\delta\boldsymbol{p} = \delta\boldsymbol{z} \tag{26}$$

where $\boldsymbol{T}$ is the combined sensitivity matrix. The inclusion of closed-loop eigenvalues results in the increased measurement data and the change of sensitivity matrix. Measurement number increases through the use of feedback loops, whereas the number of updating parameters does not change. This means that the deficiency of reliable measurements can be overcome by the use of feedback loops. We can change the eigenvalue sensitivity by the use of the feedback loop as well. If we design the feedback controller properly, the condition of combined sensitivity matrix $\boldsymbol{T}$ can be improved as the structural modification by the feedback loop changes the eigenvalue sensitivity to each parameter. For this reason, the control-loop design is very important.

IV. Control-Loop Design

Control-loop design comprises the selection of sensor and exciter locations and associated feedback gains. The characteristics of closed-loop modal data should be checked to achieve aforementioned goals. By using modal data sensitivity to a feedback gain, we will check approximate properties of the closed-loop modal data.

A. Characteristics of Closed-Loop Modal Data

Let us consider the case where accelerometers are used as output sensors for control loop. Feedback gain matrices are formulated as follows:

$$\boldsymbol{m}_f = [g_1 \quad g_2 \quad \cdots \quad g_n], \qquad \boldsymbol{c}_f = 0, \qquad \boldsymbol{k}_f = 0 \tag{27}$$

where g_s is the feedback gain corresponding to the accelerometer located in sth degree of freedom (DOF). Then the mass and stiffness

matrices change by the feedback loop addition as follows:

$$\boldsymbol{M}_f = \bar{\boldsymbol{M}} + \boldsymbol{b}\boldsymbol{m}_f = \bar{\boldsymbol{M}} + \begin{bmatrix} 0 & \cdots & 0 & \cdots & 0 \\ \vdots & & & & \vdots \\ g_1 & g_2 & \cdots & & g_n \\ \vdots & & & & \vdots \\ 0 & \cdots & 0 & \cdots & 0 \end{bmatrix} \tag{28}$$

$$\boldsymbol{K}_f = \bar{\boldsymbol{K}} \tag{29}$$

where $\bar{\boldsymbol{M}}$ and $\bar{\boldsymbol{K}}$ are system matrices including armature mass and spring stiffness of the exciter in Eqs. (17) and (18). Changes in the mass matrix are concentrated on the ath row where the exciter is attached. Let us consider the partial differentiation of system matrices with respect to g_s to estimate modal data changes.

$$\frac{\partial \boldsymbol{M}_f}{\partial g_s} = \begin{bmatrix} 0 & \cdots & 0 & \cdots & 0 \\ \vdots & & & & \vdots \\ 0 & \cdots & 1 & \cdots & 0 \\ \vdots & & & & \vdots \\ 0 & \cdots & 0 & \cdots & 0 \end{bmatrix}, \qquad \frac{\partial \boldsymbol{K}_f}{\partial g_s} = 0 \tag{30}$$

All elements of $\partial \boldsymbol{M}_f / \partial g_s$ except the element (a, s) are zero. Using these equations, the modal sensitivity to feedback gain g_s is computed. Feedback gain g_s corresponds to the sensor output located in sth DOF:

$$\frac{\partial \lambda_t}{\partial g_s} = W_t^T \left(\frac{\partial \boldsymbol{K}_f}{\partial g_s} - \lambda_t \frac{\partial \boldsymbol{M}_f}{\partial g_s} \right) W_t$$

$$= -W_t^T \lambda_t \frac{\partial \boldsymbol{M}_f}{\partial g_s} W_t = -\lambda_t W_{\text{ta}} W_{\text{ts}} \tag{31}$$

where subscript t is used to denote the target mode we want to move. The change of target eigenvalue λ_t is proportional to values of target mode shape W_t at sensor location W_{ts} and the exciter location W_{ta}. Sensitivity of target mode shape W_t for the linear model with distinct eigenvalues can be derived in the same way using the well-known equation of mode-shape sensitivity.[1,2]

$$\frac{\partial W_t}{\partial g_s} = \sum_{j=1, j\neq t}^{n} \frac{W_j W_j^T}{\lambda_t - \lambda_j} \left(\frac{\partial \boldsymbol{K}_f}{\partial g_s} - \lambda_t \frac{\partial \boldsymbol{M}_f}{\partial g_s} \right) W_t - \frac{1}{2} W_t W_t^T \frac{\partial \boldsymbol{M}_f}{\partial g_s} W_t$$

$$= \left(\sum_{j=1, j\neq t}^{n} \frac{\lambda_t W_{ja}}{\lambda_t - \lambda_j} W_j - \frac{1}{2} W_{\text{ta}} W_t \right) W_{\text{ts}} \tag{32}$$

From Eqs. (31) and (32), we can estimate closed-loop modal data with single-sensor feedback assuming a small feedback gain ($g_s \ll 1$).

$${}_c\lambda_t \simeq \lambda_t - \lambda_t W_{\text{ta}} W_{\text{ts}} g_s \tag{33}$$

$${}_cW_t \simeq W_t + \frac{\partial W_t}{\partial g_s} g_s$$

$$= \left(1 - \frac{g_s}{2} W_{\text{ta}} W_{\text{ts}} \right) W_t + g_s \lambda_t \sum_{j=1, j\neq t}^{n} \frac{W_{\text{ja}} W_{\text{ts}}}{\lambda_t - \lambda_j} W_j \tag{34}$$

The subscript c is used to designate closed-loop data. The closed-loop modal data using multiple sensors can also be derived in a similar way. Let us consider the case where m sensors are used:

$$\boldsymbol{m}_f = \begin{bmatrix} g_{s_1} & g_{s_2} & \cdots & g_{s_m} \end{bmatrix} D_s = G^T D_s \tag{35}$$

where D_s is a $m \times n$ boolean matrix for sensor locations. All elements in the jth column of D_s are zero except at the jth sensor location. Gradients of λ_t about multiple sensor locations are obtained as

$$\frac{\partial \lambda_t}{\partial G} = \begin{bmatrix} \frac{\partial \lambda_t}{\partial g_{s_1}} & \frac{\partial \lambda_t}{\partial g_{s_2}} & \cdots & \frac{\partial \lambda_t}{\partial g_{s_m}} \end{bmatrix}^T$$

$$= -\lambda_t W_{\text{ta}} \begin{bmatrix} W_{\text{ts}_1} & W_{\text{ts}_2} & \cdots & W_{\text{ts}_m} \end{bmatrix}^T \tag{36}$$

Using Eq. (36), approximate closed-loop natural frequency is derived as

$${}_c\lambda_t \simeq \lambda_t + \frac{\partial \lambda_t}{\partial G^T} G = \lambda_t - \lambda_t W_{\text{ta}} \sum_{k}^{m} W_{\text{ts}_k} g_{s_k} \tag{37}$$

In the same way, the closed-loop mode shape for multiple sensor locations can be obtained based on Eq. (34) as

$${}_cW_t \simeq W_t + \frac{\partial W_t}{\partial G^T} G = \left(1 - \frac{1}{2} W_{\text{ta}} \sum_{k=1}^{m} W_{\text{ts}_k} g_{s_k} \right) W t$$

$$+ \sum_{k=1}^{m} \sum_{j=1, j\neq t}^{n} \frac{\lambda_t W_{\text{ja}} W_{\text{ts}_k}}{\lambda_j - \lambda_t} W_j g_{s_k} \tag{38}$$

Note that closed-loop modal data are closely related to mode-shape values at sensor and exciter locations. If the mode-shape value at the sensor location is large, the modal data change becomes relatively large with the same feedback gain. The closed-loop eigendata derived in this section do not apply for the system with repeated eigenvalues. Modal sensitivity for repeated eigenvalues should be used to calculate perturbed closed-loop modal data and that case is not considered in this paper.

B. Sensor and Exciter Location

If the closed-loop system has different modal sensitivities from the original ones, the independence of closed-loop modal data from original ones can be achieved through proper selection of sensor locations and gain allocation for each sensor. The level of modal sensitivity independency is reflected in the condition number of the combined sensitivity matrix. If the condition number of the combined sensitivity matrix is low, closed-loop modal data are highly independent from the original ones, and vice versa. By inspecting Eqs. (22) and (25), we can notice that the eigenstructure should be changed from the original ones to enhance the condition of the combined sensitivity matrix. As it is rather difficult to change all modes in the frequency range of interest, each control-loop design is devoted to change a specific target mode. As shown in Fig. 3, control loops 1 and 2 are designed to change modes 1 and 2, respectively. The design sequence of control loop is shown in Fig. 4. Let us try to find the proper sensor location by using following criteria that represent the degree of change in eigenstructure.

$$C_1 = {}_c\lambda_t - \lambda_t, \qquad C_2 = W_t^T \boldsymbol{M} ({}_cW_t - W_t) \tag{39}$$

Using Eqs. (33) and (34), the criteria can be simplified for the case of a single sensor.

$$C_1 = \lambda_t W_{\text{ta}} W_{\text{ts}} g_s, \qquad C_2 = \tfrac{1}{2} W_{\text{ta}} W_{\text{ts}} g_s \tag{40}$$

$$\mathbf{T} = \begin{bmatrix} \begin{bmatrix} \mathbf{S}^0(\lambda_1, \lambda_2, \lambda_3) \end{bmatrix} \\ \begin{bmatrix} \mathbf{S}^1({}_c\lambda_1) \end{bmatrix} \\ \begin{bmatrix} \mathbf{S}^2({}_c\lambda_2) \end{bmatrix} \\ \vdots \end{bmatrix} \begin{matrix} \leftarrow \text{Open loop} \\ \leftarrow \text{Closed loop 1} \\ \leftarrow \text{Closed loop 2} \end{matrix}$$

Fig. 3 Development of combined sensitivity matrix.

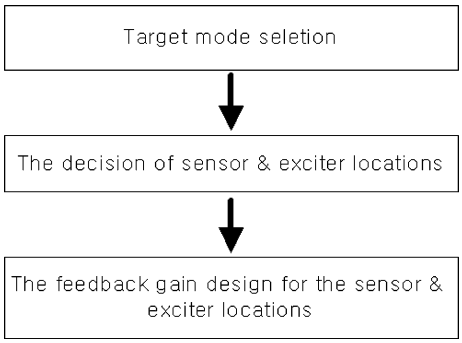

Fig. 4 Design sequence of control loop.

Note that placing sensors and exciters at the points with high mode-shape values induces large modal changes. This means that antinodal points are efficient candidates for sensor and exciter locations to change the corresponding eigenstructure.

C. Feedback Gain Design

If we use just a single-sensor location, the proper sensor location is the point where C_1 and C_2 have the largest value. And the design of feedback gain corresponding to the sensor location is not necessary. We just increase or decrease the gain until the mode is changed moderately without breaking system stability. But there can be some limits on the range the mode can be changed using single sensor. With multiple sensor points where C_1 and C_2 have relatively large values, modal change extents depends on the feedback gain allocation for each sensor. Previous research[12] about static output feedback controller dealt with methods to obtain the feedback gain vector minimizing the system energy of initial states. This type of control object is not a proper choice in changing some modes largely because the goal of conventional controllers is to minimize the system energy not to change some modes. Then we have to make new criteria for the new control purpose. The following list shows major issues that need to be addressed:

1) The feedback gain vector for selected sensor locations should accomplish predefined modal change.

2) Required control power should be minimized.

3) The norm of control gain vector should be restricted for system stability.

To define the performance index satisfying upper issues, control power should be defined. For theoretical derivation, the computation of control power is needed. We used proportional damping assumption to compute the control power of each mode. The linear system model defined in Eq. (1) can be transformed to modal coordinates using the relation between the displacement and the modal displacement.

$$\boldsymbol{x} = W\eta \tag{41}$$

$$\ddot{\eta}(t) + \boldsymbol{C}'\dot{\eta}(t) + \Lambda\eta(t) = \boldsymbol{N}(t) \tag{42}$$

where η and $\boldsymbol{N}$ are modal coordinate and modal force, respectively. $\boldsymbol{N}$ and $\boldsymbol{C}'$ are defined using mode-shape matrix W as follows:

$$\boldsymbol{N} = W^T\boldsymbol{f}, \qquad \boldsymbol{C}' = W^T\boldsymbol{C}W \tag{43}$$

With the assumption of proportional viscous damping, the system equation can be decoupled into individual modal equation.

$$\ddot{\eta}_i(t) + 2\zeta_i\omega_i\dot{\eta}_i(t) + \omega_i^2\eta(t) = N_i(t) \qquad i = 1, 2, \ldots, n \tag{44}$$

$$N_i(t) = W_i^T\boldsymbol{f}(t) = W_i^T\boldsymbol{b}f(t) = W_{\text{ia}}f(t) \tag{45}$$

$$f(t) = \frac{\mu_F r(t)}{1 + (\omega/\omega_a)j} \tag{46}$$

where W_i is the ith mode-shape vector and W_{ia} is the mode-shape value at the exciter location. Band-limited excitation force f is assumed to be a first order system with cutoff frequency ω_a as in Eq. (46). Assuming l modes are excited and m accelerometers are used to measure the vibration, the control force is expressed as follows:

$$f_c = G^T D_s\ddot{\boldsymbol{x}}(t) = G^T D_s W\ddot{\eta}(t) = G^T\hat{W}\ddot{\eta}(t) \tag{47}$$

$$\hat{W} = D_s W \tag{48}$$

where G is $m \times 1$ feedback gain vector and D_s is $m \times n$ sensor location matrix. W is $n \times l$ mode-shape matrix and η is $l \times 1$ modal coordinate vector. $\hat{W}$ is the mode-shape matrix in sensor locations. Assuming small feedback gains, the expression of control power leads to

$$E\left[f_c^2\right] = E[\ddot{\eta}^T\hat{W}^T GG^T\hat{W}\ddot{\eta}]$$

$$= tr[\hat{W}^T GG^T\hat{W}\Omega] = tr[G^T QG] \tag{49}$$

where modal power matrix Ω is defined as

$$\Omega = E[\ddot{\eta}\ddot{\eta}^T] = \text{diag}\left(E\left[\ddot{\eta}_1^2\right], E\left[\ddot{\eta}_2^2\right], \ldots, E\left[\ddot{\eta}_l^2\right]\right) \tag{50}$$

Let us consider the vibration power of each modal coordinate. The transfer function from the reference signal r in Eq. (15) to each modal coordinate $\ddot{\eta}_i$ is in the form of

$$H = \frac{(j\omega)^2}{(j\omega)^2 + 2\zeta_i(j\omega) + \omega_i^2} \cdot \frac{\mu_F W_{\text{ia}}}{1 + (j\omega)/\omega_a} \tag{51}$$

The vibration power of each modal coordinate is computed as[13]

$$E\left[\ddot{\eta}_i^2\right] = \int_{-\infty}^{\infty} |H|^2 S_r \, \mathrm{d}\omega = \frac{\pi(2\zeta_i + \omega_i/\omega_a)\omega_a\mu_F^2 W_{\text{ia}}^2 S_r}{2\zeta_i\left(1 + \omega_i^2/\omega_a^2\right) + 4\zeta_i^2 \cdot \omega_i/\omega_a}$$

$$\simeq \frac{\pi(2\zeta_i + \omega_i/\omega_a)\omega_a\mu_F^2 W_{\text{ia}}^2 S_r}{2\zeta_i\left(1 + \omega_i^2/\omega_a^2\right)} \tag{52}$$

where S_r is the power spectrum of the reference signal. The vibration power of each modal coordinate is proportional to the cutoff frequency and inversely proportional to the damping ratio. Using Eqs. (37) and (38), C_1 and C_2 for multiple sensor locations are expressed as

$$C_1 = \lambda_t W_{\text{ta}} \sum_{k=1}^{m} W_{\text{tk}} g_{s_k}, \qquad C_2 = \frac{1}{2} W_{\text{ta}} \sum_{k=1}^{m} W_{\text{tk}} g_{s_k} \tag{53}$$

As C_1 and C_2 have the same structure, we can combine them into one criterion as

$$C_t = \sum_{k=1}^{m} W_{\text{tk}} g_{s_k} = \hat{W}_t^T G \tag{54}$$

Now, the performance index satisfying the aforementioned criteria can be expressed as follows:

$$J = E\left[f_c^2\right] + \alpha(G^T G) + L(C_t - \varepsilon_t)$$

$$= tr(G^T\hat{W}\Omega\hat{W}^T G) + \alpha(G^T G) + L\left(\hat{W}_t^T G - \varepsilon_t\right) \tag{55}$$

where α is a weighting to the magnitude of feedback gain vector and L is Lagrange multiplier to include the constraint of predefined modal change ε_t. The minimization of performance index will generate a feedback gain vector that satisfies the predefined modal change.

$$G = \frac{(\hat{W}\Omega\hat{W}^T + \alpha I)^+\hat{W}_t\varepsilon_t}{\hat{W}_t^T(\hat{W}\Omega\hat{W}^T + \alpha I)^+\hat{W}_t} \tag{56}$$

$$J_{\min} = \frac{\varepsilon_t^2}{\hat{W}_t^T(\hat{W}\Omega\hat{W}^T + \alpha I)^+\hat{W}_t} \tag{57}$$

Basically, feedback gain vector has a similar shape with normal mode-shape vector $\hat{W}_t$, with a distortion by vibration power distribution Ω through modal coordinates. Ω can be thought as a kind of weighting matrix to modal power and can be allocated according to the designer's intents in real implementation. The reason we use Ω in the derivation is to clarify the effect of Ω to the feedback gain vector. In simulation example, the effect of Ω change to closed-loop system is demonstrated. If normal mode-shape matrix $\hat{W}$ estimated from measured input–output data is available and Ω is allocated properly to Eq. (55), then the feedback controller is computed directly from Eq. (56).

D. Summary

We dealt the design method of proper sensor locations and corresponding gain vectors for condition improvement of combined eigenvalue sensitivity matrix. Effective sensor and exciter locations are decided based on the perturbation of modal data by closed loop. And the associated gain vector is designed to change the target mode minimizing the control power and the norm of gain vector.

V. Simulation: Beam Thickness Estimation

Let us consider a numerical example to explain the parameter estimation process and the proposed control method. The system is a clamped-free beam with thickness variation as shown in Fig. 5. Force in vertical displacement direction is applied in a point near clamped side and the vertical displacements are measured using 10 accelerometers. Initial model for this system is constructed using the FEM with 10 elements. The initial thickness of the model is assumed constant as shown here, and thicknesses of elements 2 to 9 are going to be estimated using the five lowest measured modal data: density is 7.789×10^3 kg/m^3, length is 0.75 m, thickness is 4.8 mm, width is 0.024 m, and Young's modulus is 2.078×10^{11} N/m.

A. Open-Loop Data

To obtain input–output data, time-domain simulation is performed using MATLAB®. Noises of signal-to-noise ratio (SNR) 20dB are added to both of input and output and 8192 time-domain samples are measured using 3-kHz sampling frequency. Observer/Kalman-filter identification[14] is used to estimate impulse responses and FRF curves from noise corrupted input–output data set. From measured FRF curves or impulse responses, normal modal data are extracted using the eigensystem realization algorithm[14] and the modal data-acquisition method by Alvin.[15] The five lowest natural frequencies and associated 10×5 self-normalized mode-shape matrix are extracted. Now, the number of open-loop modal data are 55 summing up the number of natural frequencies and mode-shape matrix elements. The model and system show similar FRF shapes, but natural frequencies and mode shapes are different by the thickness variation of system from model. The modal difference between model and system are provided in Table 1 and Fig. 6. The difference of natural frequencies is definite, but the measured mode shape does

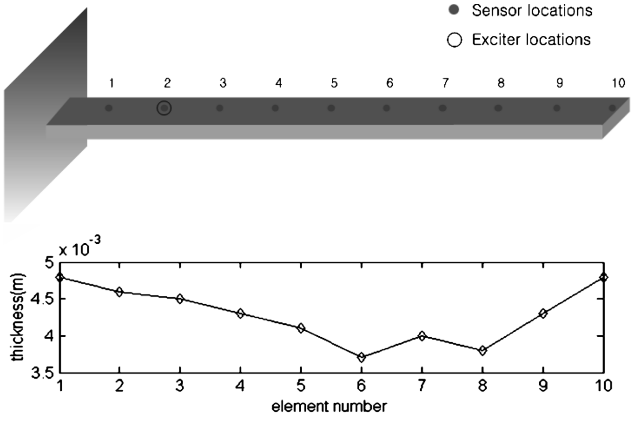

Fig. 5 Beam with thickness variations.

Table 1 Natural frequencies of model and system

Mode	Model, Hz	System, Hz
1	7.044	6.780
2	44.389	38.234
3	124.284	108.179
4	243.734	211.457
5	403.489	357.404

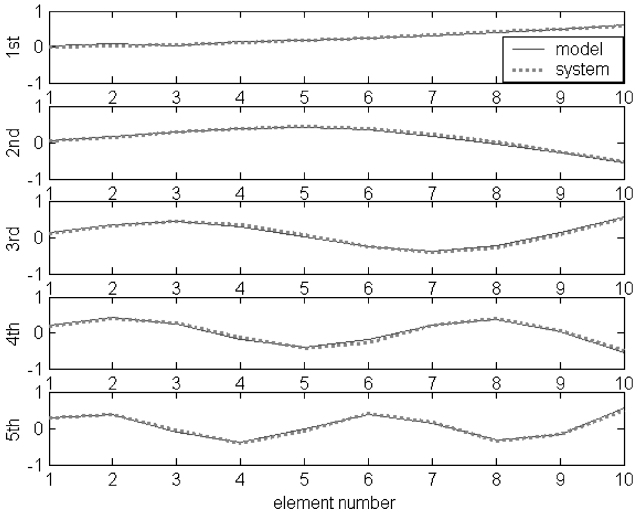

Fig. 6 Mode shapes of model and system.

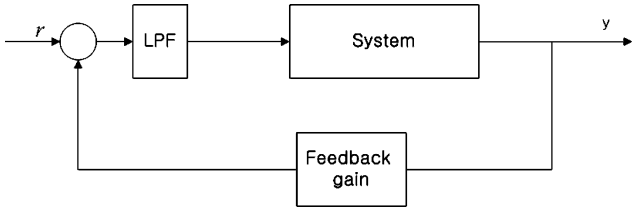

Fig. 7 Block diagram of control loop.

not show a clear difference from that of model. In this case, the effect of errors in measured mode shape can be magnified in estimated parameters, although it looks like the number of open-loop modal data are enough to estimate eight point beam thicknesses from elements 2 to 9. To avoid the use of measured mode shape, we have to generate another more data to overcome the shortage of modal data.

B. Closed-Loop Data

In this section, we will show the procedure of controller design. The block diagram of the closed-loop system is shown in Fig. 7, where a low-pass filter is introduced to prevent high-frequency modes from being driven to unstable modes. In this example, a second-order low-pass filter of cutoff frequency 1 kHz and damping ratio 0.3 is used to suppress modes above 1 kHz as the interested modes are below 600 Hz. In closed-loop simulation, seven accelerometers are attached in locations 2, 4, 6, 7, 8, 9, and 10 in Fig. 5. Ω in Eq. (50) can be thought as a kind of weighting to modal power and can be allocated according to designer's intents. Let us look at the change of closed-loop FRFs according to the allocation of Ω. The target mode is decided as the fourth mode.

$$\Omega = \mathrm{diag}(10^{-2}, 10^{-2}, 10^{-2}, 10^{-2}, 10^{-2}, 10^{-2}, 10, 10, 10)$$

$$\alpha = 1, \quad (58)$$

where modes from 1–6 are allowed to move freely as associated modal power are assigned relatively low. Figure 8 shows resulting FRFs of the closed-loop system compared to the open-loop system. Simulation condition for time-domain input–output data

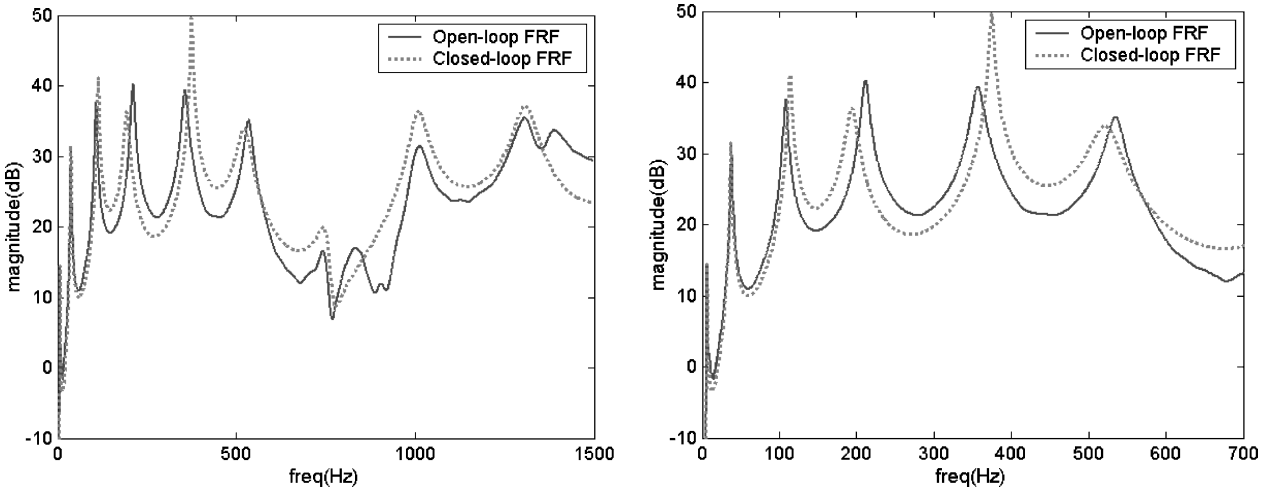

a) $H_{10,2}$ **b) Zoomed $H_{10,2}$**

Fig. 8 FRF curves of open-loop system and closed-loop system: case 1.

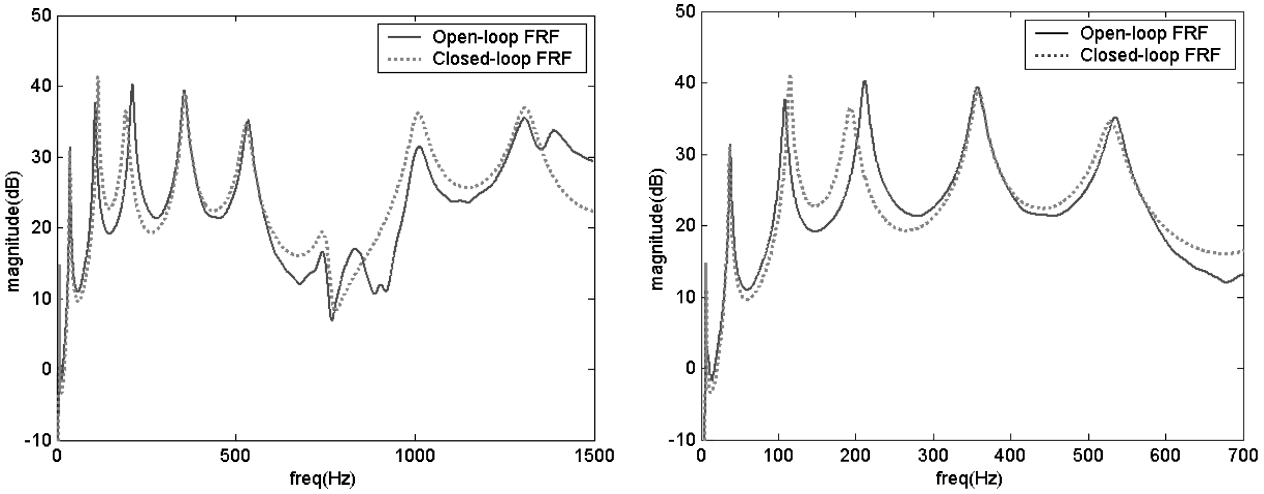

a) $H_{10,2}$ **b) Zoomed $H_{10,2}$**

Fig. 9 FRF curves of open-loop system and closed-loop system: case 2.

set and modal data-acquisition method are identical with the open-loop case. A magnitude increase of closed-loop FRF compared to open-loop FRF around 1 kHz in Fig. 8a is caused by the use of second-order low-pass filter of cutoff frequency 1 kHz. Along with the change of target mode, that is, the fourth mode in this case, other modes move too. Especially, modes 3, 5, and 6 are changed largely for we set associated modal power relatively low. Note that damping of the fifth mode is decreased from that of an open-loop system. To prevent the damping decrease of the fifth mode and maintain the stability of the closed-loop system, control power to the fifth mode should be set low to preserve the fifth mode unchanged. Then Ω is modified as

$$\Omega = \text{diag}(10^{-2}, 10^{-2}, 10^{-2}, 10^{-2}, 10, 10^{-2}, 10, 10, 10) \quad (59)$$

Resulting FRFs in Fig. 9 show that fifth mode remains unchanged. We can see what role Ω does in controller design. To verify the change of control force according to Ω distribution, normalized correlations between feedback gain vector G and lowest nine mode-shape vectors of case 1 in Eq. (58) and case 2 in Eq. (59) are shown in Fig. 10. Correlation of G and the fifth mode is suddenly reduced to near zero from case 1 to case 2. As you can see in Eq. (47), if the inner product of feedback gain vector G and mode-shape vector $\hat{W}_i$ of a mode is small, the control force to that mode diminishes. If system damping is severely nonproportional, the fifth mode cannot be fixed perfectly, and the change of system will be quite different from what is expected. But if system damping can be assumed to be just a little different from proportional damping, the fifth mode will move little, although it cannot be fixed perfectly. This damping assumption is quite well suited in a lightly damped system, where the proposed method can be applied without much difficulty.

C. Thickness Estimation Result and Analysis

Now, let us estimate thickness using the five lowest modal data. In an open-loop case, the number of available data are 55 summing up the five lowest natural frequencies and associated 10×5 mode-shape matrix. For the closed-loop case, five closed-loop systems are generated using the proposed controller design method and five closed-loop natural frequencies are measured in each closed-loop system. Consequently, a total of 30 natural frequencies of open- and close-loop system are available to estimate eight point thicknesses. Each closed-loop controller is designed using Ω distribution in Eq. (58) with different target mode and ϵ_t. The generated closed-loop natural frequencies are shown in Table 2. Errors in natural frequency measurements and self-normalized mode-shape measurments are computed as

$$\sigma(\omega_e) = 3.62 \times 10^{-2} \text{ Hz}, \qquad \sigma(\hat{W}_e) = 3.264 \times 10^{-3} \quad (60)$$

Table 2 Natural frequency generation through target mode changes

Mode	1	2	3	4	5
Open-loop, Hz	6.780	38.234	108.179	211.457	357.404
Closed-loop case 1	6.177	41.515	110.917	185.375	324.602
Target mode: 1st mode	(−0.603)	(+3.281)	(+2.738)	(−26.082)	(−32.802)
Closed-loop case 2	6.821	34.923	119.966	183.341	350.836
Target mode: 2nd mode	(+0.041)	(−3.311)	(+11.787)	(−28.116)	(−6.567)
Closed-loop case 3	6.782	39.237	95.224	222.046	351.940
Target mode: 3rd mode	(+0.002)	(+1.003)	(−12.954)	(+10.589)	(−5.463)
Closed-loop case 4	6.769	37.241	113.650	193.463	374.551
Target mode: 4th mode	(−0.011)	(−0.993)	(+5.471)	(−17.995)	(+17.147)
Closed-loop case 5	6.769	38.076	107.076	222.233	325.478
Target mode: 5th mode	(−0.010)	(−0.157)	(−1.102)	(+10.775)	(−31.926)

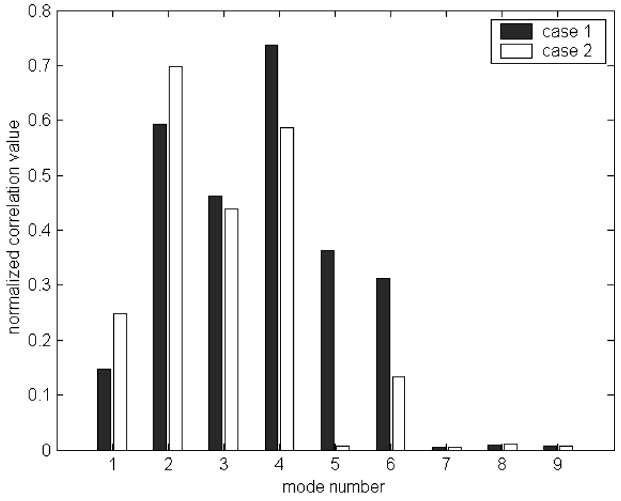

Fig. 10 Correlation between *G* and mode-shape vectors.

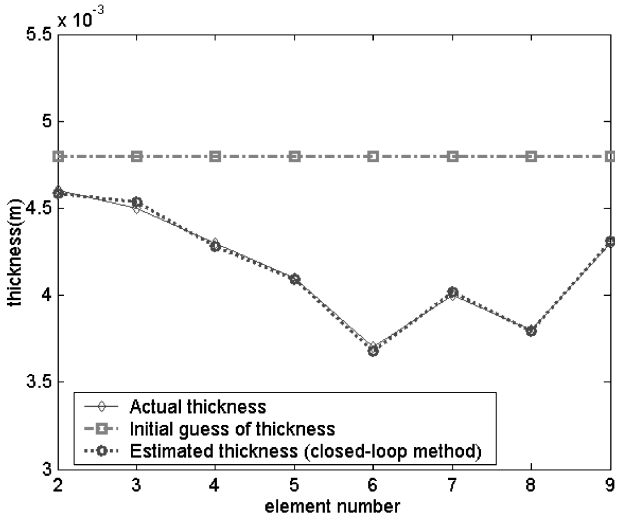

Fig. 11 Thickness estimation (closed-loop method, data number: 25).

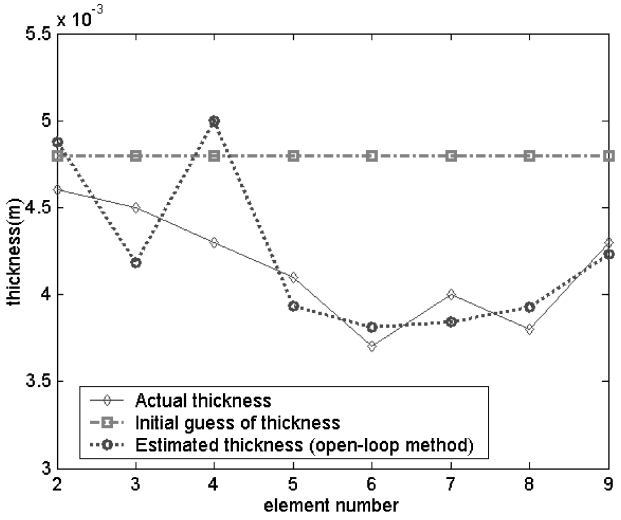

a) Data number: 25

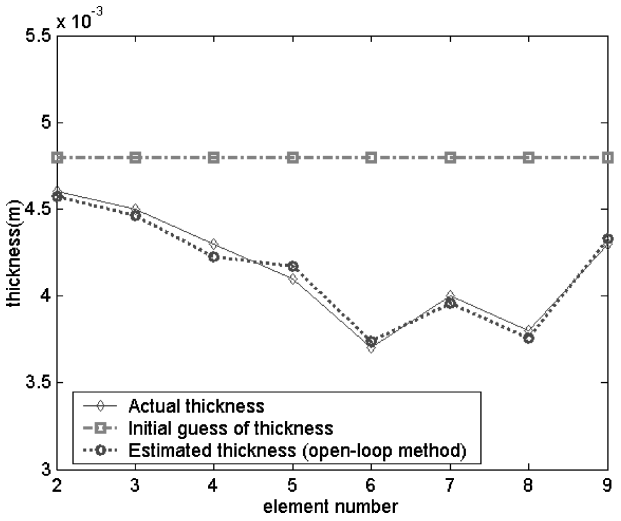

b) Data number: 45

Fig. 12 Thickness estimation (open-loop method).

where σ is standard deviation and subscript e is used to denote measurement error. To compare open- and closed-loop cases, five open-loop natural frequencies and 20 closed-loop natural frequencies are used in the closed-loop case, whereas five open-loop natural frequencies and 20 normal mode-shape values are used in the open-loop case. Estimated parameters using 25 open- and closed-loop natural frequency measurements converge to actual thickness distribution as shown in Fig. 11, whereas estimated parameters using 25 open-loop modal data in Fig. 12a show a large deviation from the actual thickness distribution. The performance difference is caused as normal mode-shape measurements are contaminated by many more errors than natural frequency measurements. Basically, natural frequency measurements carry fewer errors as a natural frequency is estimated using all meausured FRFs, whereas a single element of a mode-shape vector is caculated from a single FRF. Even more, many processes such as mode-shape expansion and normalization are required to extract normal mode shapes from measured FRFs, and these bring error contamination in normal mode shapes. To achieve a performance similar to Fig. 11, much more data are required in the open-loop case as shown in Fig. 12b. To compare the estimation performance of the open-loop method and the closed-loop method, the error norm of estimated thicknesses are plotted according to data

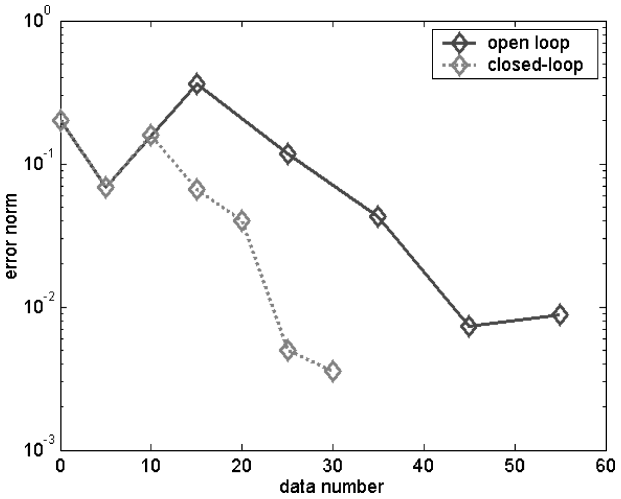

a) Error norm according to data number

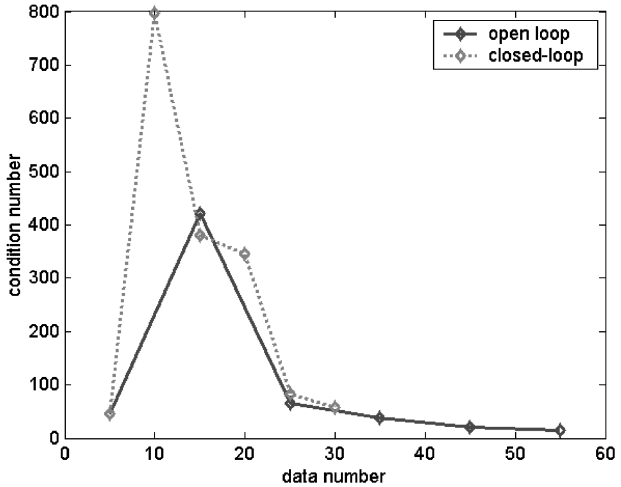

b) Condition number of sensitivity matrix

Fig. 13 Comparison of open- and closed-loop method.

number in Fig. 13a, and the associated condition number of the sensitivity matrix according to the data number is shown in Fig. 13b. Much more data are required for the open-loop method to achieve a similar estimation performance of the closed-loop method. This result shows one benefit of the proposed method. We can get a reliable estimation result with a smaller number of data. This result comes from the fact that we can generate less contaminated natural frequency measurements through diverse construction of intentional closed-loop systems.

VI. Conclusions

In this research, a novel concept that introduces feedback loop from sensors to exciter of conventional modal test setup is proposed. This method uses closed-loop modal data to overcome the problems of the conventional sensitivity-based method in parameter modification of the linear model. At first, new energy paths generated by the feedback loop change the modal characteristics of the system, and these additional closed-loop modal data can solve the problem caused by the deficiency of the modal data. Secondly, the feedback loop alternates modal sensitivities of parameters. Through the feedback loop, we can change similar modal sensitivities of some parameters and consequently achieve better estimation of parameters. We derived approximate closed-loop modal data as a function of sensor locations and associated feedback gain. Based on these properties, we proposed a design method of static output feedback controller for noncollocated sensor and exciter set. The proposed controller is efficient in changing target modes. Simulation studies about the parameter estimation performance of conventional methods and the proposed method show that we can achieve better estimation performance with a smaller number of data.

Appendix: Closed-Loop Eigenvalue Sensitivity

The closed-loop system has the following biorthogonality:

$$\boldsymbol{K}_f W^R = \boldsymbol{M}_f W^R \Lambda_c \tag{A1}$$

$$\boldsymbol{K}_f^T W^L = \boldsymbol{M}_f^T W^L \Lambda_c \tag{A2}$$

$$(W^L)^T \boldsymbol{K}_f W^R = \Lambda_c, \qquad (W^L)^T \boldsymbol{M}_f W^R = I \tag{A3}$$

From Eq. (A1), the following equation holds for tth eigenvalue:

$$\left(W_t^L\right)^T (\boldsymbol{K}_f - {}_c\lambda_t \boldsymbol{M}_f) W_t^R = 0 \tag{A4}$$

Differentiating both sides of Eq. (A4) with jth updating parameter results in

$$\frac{\partial \left(W_t^L\right)^T}{\partial \theta_j} (\boldsymbol{K}_f - {}_c\lambda_t \boldsymbol{M}_f) W_t^R + \left(W_t^L\right)^T \frac{\partial (\boldsymbol{K}_f - {}_c\lambda_t \boldsymbol{M}_f)}{\partial \theta_j} W_t^R + \left(W_t^L\right)^T (\boldsymbol{K}_f - {}_c\lambda_t \boldsymbol{M}_f) \frac{\partial W_t^R}{\partial \theta_j} = 0 \tag{A5}$$

From Eqs. (A1) and (A2), the first and third terms in Eq. (A5) are 0, and we can simplify Eq. (A5) as

$$\frac{\partial (\boldsymbol{K}_f - {}_c\lambda_t \boldsymbol{M}_f)}{\partial \theta_j} = \frac{\partial \boldsymbol{K}_f}{\partial \theta_j} - \frac{\partial {}_c\lambda_t}{\partial \theta_j} \boldsymbol{M}_f - {}_c\lambda_t \frac{\partial \boldsymbol{M}_f}{\partial \theta_j} \tag{A6}$$

Multiplying $(W_t^L)^T$ in the left side and W_t^R in the right side of Eq. (A6) results in

$$\begin{aligned} \left(W_t^L\right)^T \frac{\partial (\boldsymbol{K}_f - {}_c\lambda_t \boldsymbol{M}_f)}{\partial \theta_j} W_t^R &= \left(W_t^L\right)^T \frac{\partial \boldsymbol{K}_f}{\partial \theta_j} W_t^R \\ &- \left(W_t^L\right)^T \frac{\partial {}_c\lambda_t}{\partial \theta_j} \boldsymbol{M}_f W_t^R - {}_c\lambda_t \left(W_t^L\right)^T \frac{\partial \boldsymbol{M}_f}{\partial \theta_j} W_t^R \\ &= \left(W_t^L\right)^T \frac{\partial \boldsymbol{K}_f}{\partial \theta_j} W_t^R - \frac{\partial {}_c\lambda_t}{\partial \theta_j} - {}_c\lambda_t \left(W_t^L\right)^T \frac{\partial \boldsymbol{M}_f}{\partial \theta_j} W_t^R = 0 \end{aligned} \tag{A7}$$

Then closed-loop eigenvalue sensitivity is derived as

$$\frac{\partial {}_c\lambda_t}{\partial \theta_j} = \left(W_t^L\right)^T \left(\frac{\partial \boldsymbol{K}}{\partial \theta_j} - {}_c\lambda_t \frac{\partial \boldsymbol{M}}{\partial \theta_j} \right) W_t^R \tag{A8}$$

Acknowledgments

This work was supported by the National Research Laboratory Program (2000-N-NL-01-C-148) and the Brain Korea 21 project of the Republic of Korea in 2003.

References

[1]Mottershead, J. E., and Friswell, M. I., "Model Updating in Structural Dynamics: A Survey," *Journal of Sound and Vibration*, Vol. 167, No. 2, 1993, pp. 347–375.

[2]Friswell, M. I., *Finite Element Model Updating in Structural Dynamics*, 1st ed., Kluwer Academic, London, 1996, Chap. 5.

[3]Dascotte, E., "Practical Application of Finite Element Tunning Using Experimental Modal Data," *Proceedings of the 8th International Modal Analysis Conference*, Vol. 2, edited by D. J. Demichele, Society for Experimental Mechanics, Bethel, CT, 1990, pp. 1032–1037.

[4]D'Ambrogio, W., and Fregolent, A., "The Use of Antiresonances for Robust Model Updating," *Journal of Sound and Vibration*, Vol. 236, No. 2, 2000, pp. 227–243.

[5]Li, S., Shelly, S., and Brown, D., "Perturbed Boundary Condition Testing," *Proceedings of the 13th International Modal Analysis Conference*, Vol. 1, edited by D. J. Demichele, Society for Experimental Mechanics, Bethel, CT, 1995, pp. 902–907.

[6]Nalitolela, N. G., Penny, J. E. T., and Friswell, M. I., "A Mass or Stiffness Addition Technique for Structural Parameter Updating," *International Journal of Analytical and Experimental Modal Analysis*, Vol. 7, No. 3, 1992, pp. 157–168.

[7]Cha, P. D., and Gu, W., "Model Updating Using an Incomplete Set of Experimental Modes," *Journal of Sound and Vibration*, Vol. 233, No. 4, 2000, pp. 587–600.

[8]Gordis, J. H., "Artifcial Boundary Conditions for Model Updating and Damage Detection," *Mechanical Systems and Signal Processing*, Vol. 13, No. 3, 1999, pp. 437–448.

[9]Nalitolela, N. G., Penny, J. E. T., and Friswell, M. I., "Updating Model Parameters by Adding an Imagined Stiffness to the Structure," *Mechanical Systems and Signal Processing*, Vol. 7, No. 2, 1993, pp. 161–172.

[10]Lew, J. N., and Juang, J. N., "Structural Damage Detection Using Virtual Passive Controllers," *Journal of Guidance, Control, and Dynamics*, Vol. 25, No. 3, 2002, pp. 419–424.

[11]Rothwell, E., and Blischke, M. A., "A Unified Approach to Solving Ill-Conditioned Matrix Problems," *International Journal for Numerical Methods in Engineering*, Vol. 28, 1989, pp. 609–620.

[12]Syrmos, V. L., Abdallah, C. T., Dorato, P., and Grigoriadis, K., "Static Output Feedback—A Survey," *Automatica*, Vol. 33, No. 2, 1997, pp. 125–137.

[13]Newland, D. E., *An Introduction to Random Vibrations, Spectral & Wavelet Analysis*, 1st ed., Wiley-Interscience, New York, 1993, Chap. 7.

[14]Juang, J.-N., *Applied System Identification*, Prentice–Hall, Upper Saddle River, NJ, 1994, Chaps. 5 and 6.

[15]Alvin, K. F., and Park, K. C., "Second-Order Structural Identification Procedure via State-Space-Based System Identification," *AIAA Journal*, Vol. 32, No. 2, 1994, pp. 397–406.